Carbohydrate Polymers 110 (2014) 47–52

Contents lists available at ScienceDirect

Carbohydrate Polymers

journal homepage: www.elsevier.com/locate/carbpol

Cellulose nanofibril based graft conjugated polymer films act as a chemosensor for nitroaromatic

Qingyuan Niu, Kezheng Gao, Wenhui Wu*

School of Materials Science & Engineering, Beijing Institute of Technology, Beijing 100081, PR China

ARTICLE INFO

Article history:
Received 3 December 2013
Received in revised form 25 January 2014
Accepted 2 March 2014
Available online 27 March 2014

Keywords:
Cellulose nanofibril
Conjugated polymer
Chemical assembly
Fluorescent sensor
Nitroaromatic

ABSTRACT

A cellulose nanofibril film is modified by chemical assembly of boronate-terminated conjugated polymer chains at its specific sites, C-6 carboxyl groups. The modified cellulose nanofibril film is used as a fluorescent sensor for nitroaromatic vapor. Thanks to the specific reactive sites, numerous loose cavities or pathways located in the film sensor's out-layer have been formed, and the fraction of easily accessible cavities of the novel fluorescent film sensor is up to 0.97, which could benefit the penetration and diffusion of analyte vapor. Therefore, the novel fluorescent film sensor exhibits high sensitivity toward nitroaromatic vapor with a fast response. The fluorescence quenching efficiency of the chemical-assembly film sensor is about 3 times larger than that of the spin-cast film sensor using the same conjugated polymer for 600 s exposure to DNT vapor. In addition, the novel fluorescent film sensor shows good reversibility.

1. Introduction

The fast and sensitive detection of explosives is of crucial significance for security checking of the explosives in airport or other public sites, land-mine detection, and so on (Che et al., 2012; Lan et al., 2009; Tao, Li, & Zhu, 2006; Wang, La, Ding, Liu, & Lei, 2012; Yang, Turnbull, & Samuel, 2010; Zhang, Lu, Gao, Ding, & Fang, 2007; Zhu et al., 2011). Currently, conjugated polymers (CPs) have been explored as optoelectronic sensor for the detection of trace nitroaromatic-based explosives, such as 2,4,6-trinitrotoluene (TNT) and 2,4-dinitrotoluene (DNT), because the CPs backbones could display the fluorescent amplification or superquenching effects toward analytes (Thomas, Joly, & Swager, 2007). Therefore, numerous investigations have emphasized on the design and synthesis of CPs with various structures to detect nitroaromatic vapor (Basabe-Desmonts, Reinhoudt, & Crego-Calama, 2007; Feng, Li, & Yang, 2010; He, Zhang, Lue, & Fang, 2009; Long et al., 2009; Narayanan, Varnavski, Swager, & Goodson, 2008). In pioneering work developed by Swager's group, the pentiptycene-based fluorescent polymer film was an example of a highly sensitive vapor phase sensor (Yang & Swager, 1998). The incorporation of bulky and rigid three-dimensional pentiptycene moieties could prevent aggregation and self-quenching, and create the "molecular pore" in spin-cast film to benefit the penetration of the explosive vapor. Nevertheless, the sensing performance of most spin-cast sensors is heavily relied on the film thickness (Wang et al., 2012). To achieve a measurable intensity of the fluorescence signal, a sufficiently thick film is usually required, while the presence of an internal layer of a conjugated polymer film unpenetrated and unquenched by the explosive vapors would decrease the quenching efficiency. Moreover, the preparation of CPs-based spin-cast sensors with various structures needs sophisticated chemical modification or polymer backbone/side-chain functionalization.

2,2,6,6-tetramehylpiperidine-1-oxyl (TEMPO)-oxidized cellulose nanofibril films, CNF films, were a wise choice as ideal substrates of the chemosensors for potential application. The CNF film was prepared by selectively introducing reactive carboxyl groups on the C-6 of the cellobiose repeat unit (Fukuzumi, Saito, Wata, Kumamoto, & Isogai, 2009; Isogai, Saito, & Fukuzumi, 2011). Thus, it is easy to functionalize the CNF film, because the carboxyl groups could be reacted with amine groups in mild condition used 1-ethyl-3-(3-dimethylaminopropyl) carbodiimide (EDC) together with N-hydroxysuccinimide (NHS) as effective amidation catalyst (Follain, Marais, Montanari, & Vignon, 2010; Miao et al., 2011). The spacing of C-6 carboxyl groups on cellobiose repeat units of the cellulose chains is approximately 1.04 nm (Holt, Stoyanov, Pelan, & Paunov, 2010). In addition, the CNF film has some superior performance, such as flexibility, good portability, environmentally friendly nature, and so on (Hirota, Furihata, Saito, Kawada, & Isogai, 2010; Saito, Kimura, Nishiyama, & Isogai, 2007). Also, the raw material of CNF film, cellulose, is the most abundant organic material on

* Corresponding author. Tel.: +86 010 68912659; fax: +86 010 68912659.
E-mail addresses: niuqingyuan1984@126.com (Q. Niu), wuwh@bit.edu.cn (W. Wu).

http://dx.doi.org/10.1016/j.carbpol.2014.03.042
0144-8617/

the planet in the world (Peterson, Willgert, Hansson, Malmstrom, & Carter, 2011).

To explore a simple strategy of design and fabricating ultra-sensitive vapor-phase explosives, herein we report a novel fluorescent film was prepared by chemical assembly of boronate-terminated CPs at the C-6 carboxyl groups of CNF film surface. It is expected that in this strategy, due to the near 1.04 nm spacing of the C-6 carboxyl groups on cellobiose repeat unit as reactive grafting-to sites, numerous easily accessible cavities or loose pathways could be generated by grafted CP chains located in the chemical-assembly film sensor's surface, which could benefit the nitroaromatic vapor penetration into sensory out-layer of the film. As a result, with relatively simple chemical modification, the cellulose nanofibril based fluorescence film would therefore be proposed to be an excellent candidate for detecting nitroaromatic vapor.

2. Experimental

2.1. Materials

4-Bromobenzyl bromide, EDC, NHS, 2-(N-Morpholino) ethanesulfonic acid (MES), 9,10-diphenylanthracene, 4-bromoaniline and 2,2,6,6-tetramehylpiperidine-1-oxyl (TEMPO) were obtained from Aladdin-Reagent Co., Ltd. 3,6-Dibromocarbazole, tetrakis(triphenylphosphine) palladium ($Pd(PPh_3)_4$) and 9,9-dihexylfluorene-2,7-bis(trimethyleneborate) were purchased from SynSwitch. Other reagents and solvents obtained from commercial suppliers were used without further purification.

2.2. Instrumentation

Fourier transform infrared spectroscopy (FTIR) spectra were obtained using a Bruker TENSOR 27. Polymer powder was pressed into discs with KBr and then FTIR spectrum was measured. The FTIR spectra of film samples were measured directly. Gel permeation chromatography (GPC) was carried out on a Waters GPC515-2410 System with THF as an eluant. ^1H NMR spectrum of the solution containing 15 mg polymer powder and 5 mL $CDCL_3$ was recorded with a Bruker Avance III 600 NMR spectrometer (600 MHz). Water contact angles of the films were measured using a JC2000C1 contact-angle instrument at ambient temperature with a drop size of 0.5 μL. Contact angles were taken 1 min after droplet deposition on the surface, and averaged over three drops in various locations. UV–vis absorption and photoluminescence (PL) spectra of samples were recorded using a Shimadzu UV-1700 Ultraviolet Spectrophotometer and a Hitachi F-4500 Fluorescence Spectrophotometer, respectively.

2.3. Synthesis of boronate-terminated conjugated polymer chains (PFC)

The mixture containing 9,9-dihexylfluorene-2,7-bis(trimethyleneborate) (502 mg, 1 mmol), 3,6-dibromocarbazole (325 mg, 1 mmol), THF (15 mL) and K_2CO_3 aqueous solution (2 M, 10 mL) were stirred and degassed with N_2 for 30 min. Then $Pd(PPh_3)_4$ (24 mg, 2.0 mol%) was added under N_2. After refluxing (about 69 °C) for 48 h, the end groups were capped by heating the mixture under reflux with 9,9-dihexylfluorene-2,7-bis(trimethyleneborate) (200 mg, 0.4 mmol) for another 6 h. The mixture was cooled and poured into methanol. The precipitates were collected by filtration, and washed with abundant methanol and water, respectively, for several times. After removal of organic solvents and water, the solid was extracted with acetone for 48 h using Soxhlet apparatus. Finally, the PFC ($\bar{M}_n$: 6760, PDI: 1.49) was obtained after being dried at 40 °C under vacuum for 3 days.

2.4. Preparation of Br-containing reactive sites in CNF film surface (Br@CNF film)

The CNF films (20 mm × 20 mm, 64 mg) were immersed into MES buffer (20 mL, pH = 5.0). EDC (226 mg) and NHS (38 mg) were added and the mixture was slowly stirred for 30 min at 4 °C. Then 4-bromoaniline (177 mg) dissolved in DMF (5 mL) was added, and the mixture was stirred at room temperature. After 24 h, the Br-modified CNF films were taken out and washed twice with sequence of DMF, water and methanol. At last, the samples were used soxhlet extraction with THF for 24 h and dried in a vacuum oven.

2.5. Synthesis of PFC@CNF films

After the PFCs (800 mg) were dissolved in THF (30 mL), K_2CO_3 aqueous solution (2 M, 20 mL), the Br@CNF films (20 mm × 20 mm, 300 mg) were added. After degassing with N_2 for 30 min, $Pd(PPh_3)_4$ (24 mg) was added quickly. The reaction was then refluxed at 69 °C for 12 h. After cooling to room temperature, the PFC@CNF films were taken out and rinsed two times with sequence of THF, DCM, methanol, and water. To exclude simple entangling/physisorption of the PFC chains within the nanofiber cellulose network, the samples were used soxhlet extraction with THF for 24 h and dried in vacuo.

2.6. Preparation of PFC-modified filter paper (PFC@CELL paper)

Filter paper (20 mm × 20 mm, 0.510 g) and DMF (25 mL) were added in a 100-mL flask. The mixture was stirred and degassed with N_2 for 30 min. Then NaH (1.14 g) was added to this mixture. After 30 min, the solution of 4-bromobenzyl bromide (2.12 g) and DMF (5 mL) was added, and stirred for another 24 h. After reaction, the mixture was put into water (500 mL), Then the Br-modified filter papers were rinsed twice each with solvent following sequence of DMF, water and methanol. The Br-modified filter paper was used soxhlet extraction with methanol and dried in vacuo.

The mixture containing PFC (800 mg), THF (30 mL), K_2CO_3 aqueous solution (2 M, 20 mL), and the Br-modified filter papers (20 mm × 20 mm, 400 mg) was stirred and degassed with N_2 for 30 min. Then $Pd(PPh_3)_4$ (24 mg) was added quickly. The reaction was then performed at 69 °C for 12 h. After cooling to room temperature, the samples were rinsed two times each with THF, DCM, methanol, water and THF. The samples were then Soxhlet extracted using THF and dried under vacuum at 30 °C.

2.7. Synthesis of PFC(SC) films

The PFC solution (0.45 mg in 1 mL THF) was spin-casted onto a quartz substrate (microscope slide, length: 24 mm, width: 24 mm and thickness: 1 mm) at a spin rate of 1000 rpm. Then, the PFC(SC) films were dried at 30 °C under vacuum for 1 day.

3. Results and discussion

3.1. Synthesis and characterization

To graft conjugated polymer chains covalently onto the CNF film surface, we followed the reaction route illustrated in Scheme 1. First, 4-bromoaniline was reacted with the C-6 carboxyl groups of the CNF film surfaces through pre-activation by EDC/NHS to form Br-containing reactive sites (Br@CNF film). Next, the additional diboronate-terminated monomers were added to prepare boronate-terminated conjugated polymer. Finally, the PFCs were bonded onto the Br@CNF film surfaces via "grafting to" technique,

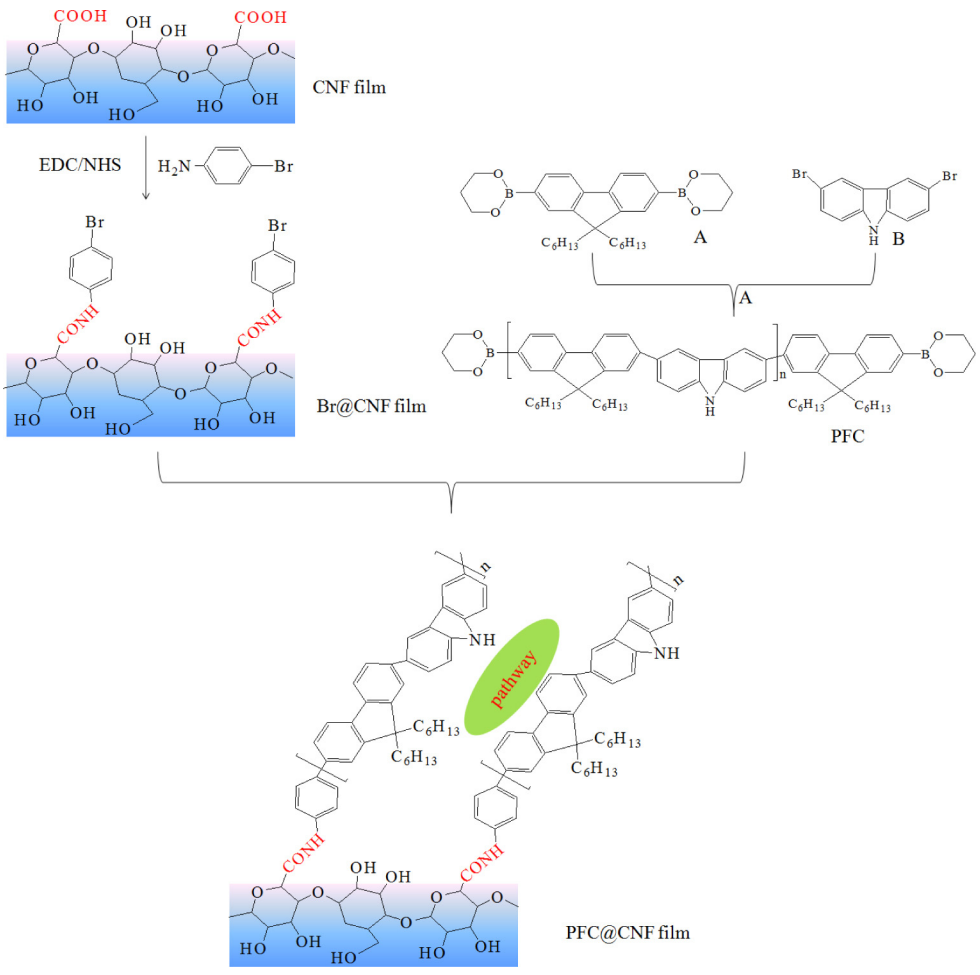

Scheme 1. Schematic of synthetic routes of PFC@CNF film.

and the PFC@CNF films were obtained. In order to minimize simple entangling/physisorption of the PFC chain within the nanofiber cellulose network, in each step after the preparation, these samples were Soxhlet extracted for 24 h.

The ^{1}H NMR spectrum of PFC is shown in Fig. 1a. The peak at 4.05 ppm assigned to the protons in the methylene end group (O—CH_2) proves the boronate termination. The PFC@CNF film, Br@CNF film and CNF film have been characterized by FT-IR and wettability measurements. Fig. 1b shows the FT-IR spectra of these films and pure PFC. The absorption band of CNF film around 1729 cm^{-1} due to stretching vibration of free carboxyl C=O groups mostly disappeared. New bands for the Br@CNF film at 1700, 1667 and 1534 cm^{-1} assigned to C=ON, C=ONH and N—HCO groups appeared, respectively. For the PFC@CNF film, the spectrum gave a significant absorption at 1607 cm^{-1}, corresponding to N—H group, while the pure PFC had the same characteristic peak at 1607 cm^{-1}.

The surface hydrophobic performance was characterized by static contact angle observation and shown in Fig. 1c. The contact angle between water drop and films was increased from 44.8 ± 0.5° to 70.7 ± 0.2° after the arylbromide modification of the CNF film. The PFC@CNF film was found to be relatively hydrophobic, showing a static contact angle of 75.2 ± 0.3°. The above observations allow us to conclude that the hydrophobic conjugated PFC chains have been successfully linked to the grafting sites in the CNF film surface.

3.2. Photophysical properties

The absorption and fluorescence spectra of the PFC@CNF film, PFC(SC) film, and PFC in THF dilute solution are shown in Fig. 2a and b. Obviously, the absorption and fluorescence maxima of the PFC(SC) film were shifted by approximately 25 nm and 32 nm to longer wavelength, respectively, compared with that of PFC in THF dilute solution (323 nm and 390 nm, respectively). However, the red shift of the absorption and fluorescence spectra for the PFC@CNF film is only 8 nm and 20 nm, respectively. The possible reason is C-6 carboxyl groups on cellobiose repeat unit of the CNF film was used as reactive grafting-to sites, resulting in loose distribution of grafting PFC chains. Such loose PFC chains structure could, to a certain extent, suppress the PFC chain aggregation effect of the PFC@CNF film, while PFC in THF dilute solution could be regarded as isolated molecular chains dispersed in solution without chain aggregation.

3.3. Fluorescence quenching characteristic of PFC@CNF film to DNT solution

The sensing property of PFC@CNF film was applied to detect nitroaromatic solution (DNT as a representative nitroaromatic). The fluorescence spectral response of the PFC@CNF film toward DNT in DMF is shown in Fig. 3a. The fluorescent intensity was remarkably decreased with the increase of DNT concentration. The quenching behavior is characterized by the Stern–Volmer equation (Eq (1)) (Wu et al., 2012):

$$\frac{I_0}{I} = 1 + K_{SV}[Q] \quad (1)$$

In Eq (1), I_0 is the fluorescence intensity in the absence of added quencher; I is the fluorescence intensity as a function of quencher

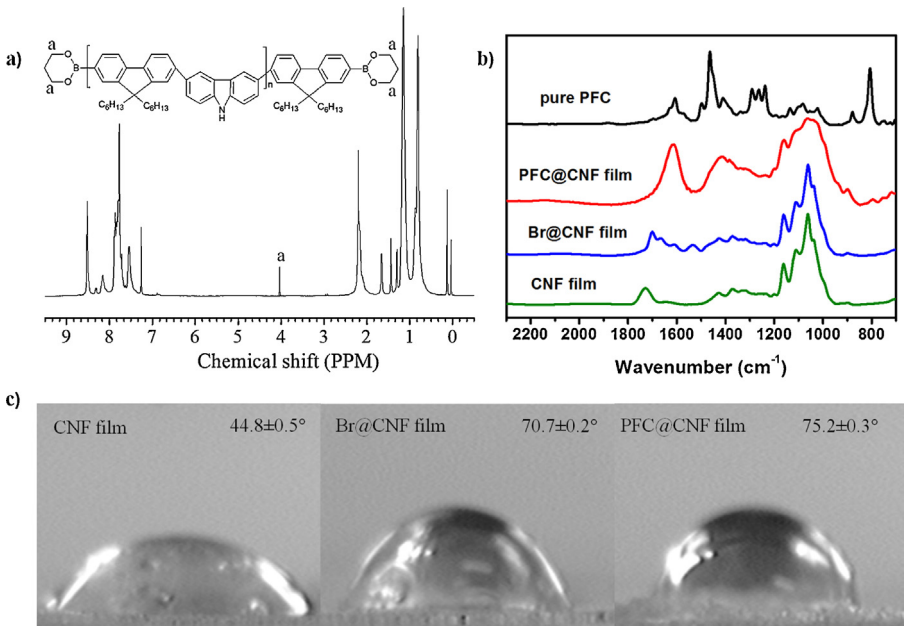

Fig. 1. (a) The ^{1}H NMR spectrum of PFC; (b) Infrared spectra of CNF film, Br@CNF film, PFC@CNF film and pure PFC; (c) the contact angle of CNF film, Br@CNF film, and PFC@CNF film.

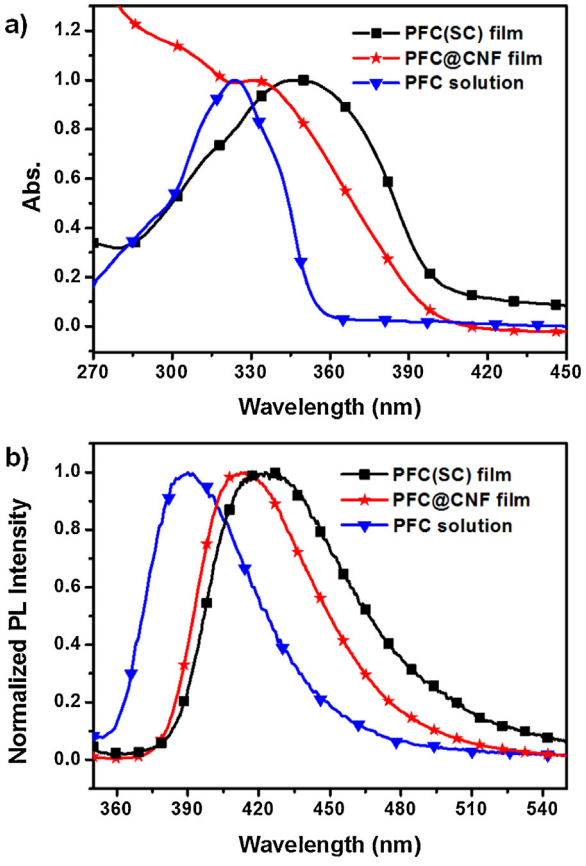

Fig. 2. (a) The absorption and (b) fluorescence spectra of PFC in THF solution, PFC@CNF film, and PFC(SC) film.

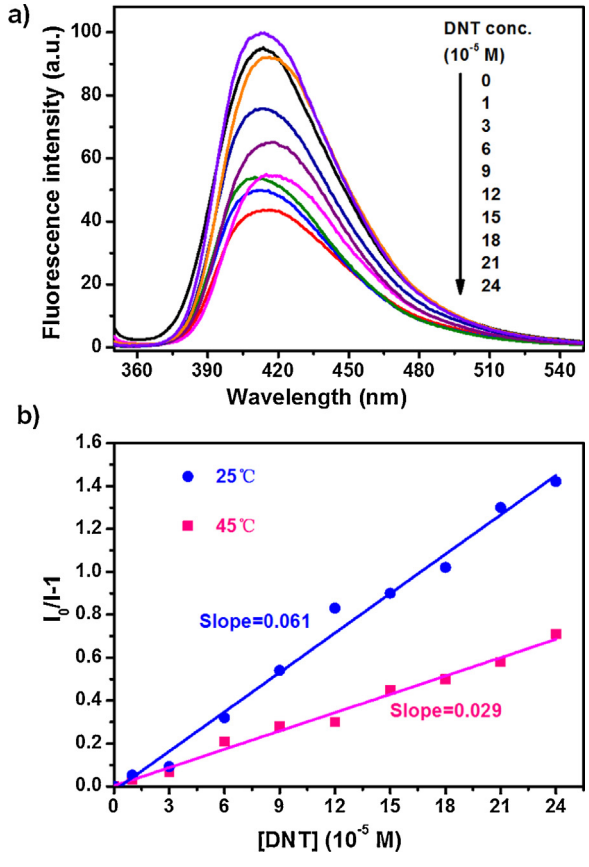

Fig. 3. (a) Fluorescence quenching characteristic of PFC@CNF film as a function of DNT concentration in DMF; (b) Stern–Volmer plots for the fluorescence quenching of PFC@CNF films by DNT in solution at 25 °C and 45 °C.

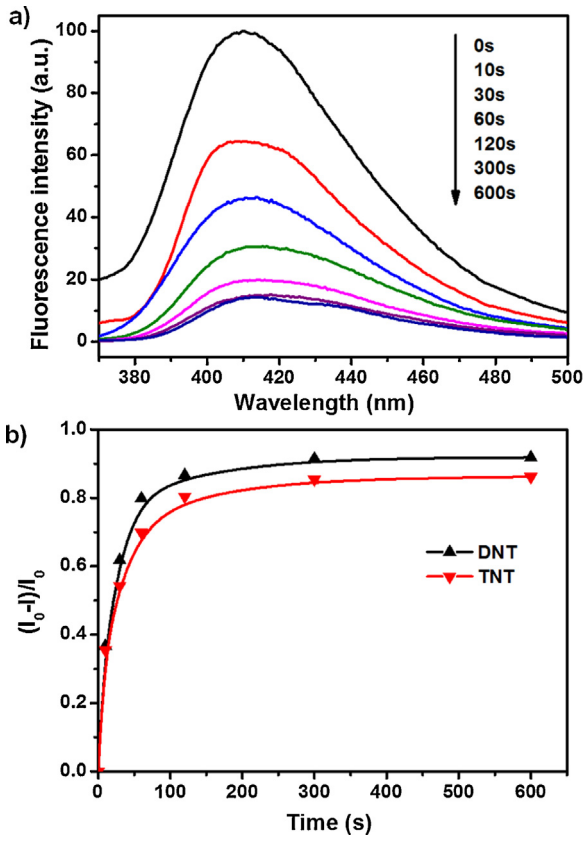

Fig. 4. (a) Time-dependent fluorescence intensities of PFC@CNF film upon exposure to saturated TNT vapor; (b) Fluorescence quenching efficiencies of PFC@CNF films upon exposure to DNT and TNT vapor at different times, respectively.

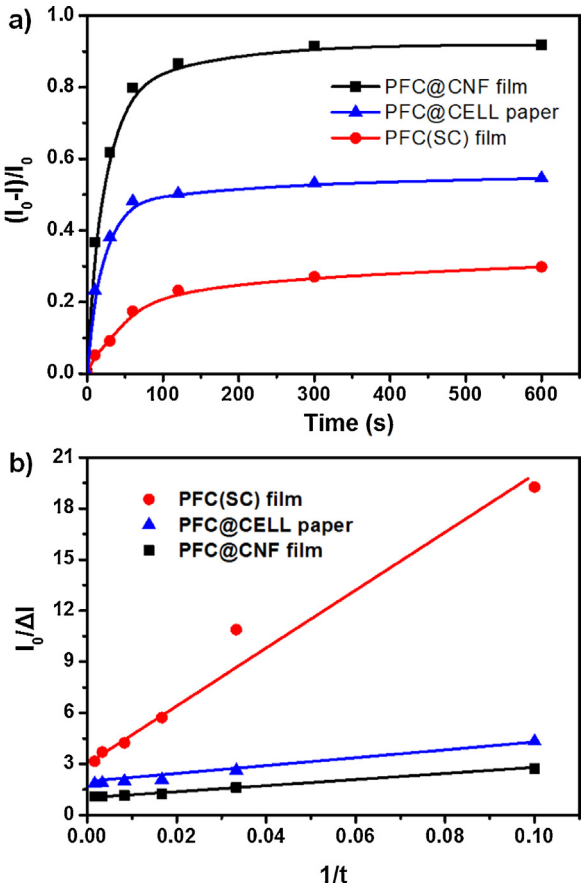

Fig. 5. (a) Fluorescence quenching efficiencies of PFC@CNF film, PFC(SC) film, and PFC@CELL paper upon exposure to DNT vapor at different times, respectively; (b) the modified Stern–Volmer plots for PFC@CNF film, PFC(SC) film, and PFC@CELL paper.

concentration [Q]. The slope of the plots gives the Stern–Volmer quenching constant (K_{SV}).

The relative emission intensities of PFC@CNF films at two different temperatures were plotted as a function of DNT concentration (Stern–Volmer plot, Fig. 3b). The quenching constants (K_{SV}) of PFC@CNF films to DNT calculated from the linear part of the Stern–Volmer plots are $6.1 \times 103\,M^{-1}$ at 25 °C, and $2.9 \times 103\,M^{-1}$ at 45 °C, respectively. These results revealed that the nature of the quenching is a static quenching. Note that the linear detection range of DNT concentrations is from 1.0×10^{-5} to 24×10^{-5} M.

3.4. Vapor-phase fluorescence quenching

The sensing performance of the PFC@CNF films was also used to detect nitroaromatic vapors (DNT or TNT were used as representative nitroaromatics.). The PFC@CNF film was inserting into sealed vials (25 mL volume) at room temperature containing solid analytes and cotton gauze, which could help to maintain a constant saturated vapor pressure and prevent the film from directly contacting the analytes. The fluorescence spectra were recorded immediately after exposing the PFC@CNF film to the analyte vapor for a specific period of time at excitation wavelength of 331 nm. A representative set of fluorescence spectra obtained for the exposure of the PFC@CNF film to TNT vapor are shown in Fig. 4a. Simultaneous fluorescence quenching was observed. Fig. 4b shows the fluorescence quenching efficiency ($(I_0 - I)/I_0$) of the PFC@CNF film to DNT and TNT, respectively. 30 s exposure to TNT would result in 54.3% reduction of the fluorescence emission. While to DNT, 30 s exposure made the reduction exceed 61.8%. Clearly, the emission of the PFC@CNF film to DNT vapor is much more sensitive than to TNT, mainly because of the higher volatility of DNT than TNT.

For comparison, the PFC(SC) film and PFC@CELL paper were also used to detect DNT vapor. The fluorescence quenching efficiencies of the PFC@CNF film, PFC(SC) film, and PFC@CELL paper to DNT vapor are shown in Fig. 5a. The fluorescence quenching efficiency of the PFC@CNF film (91.8%) is about 3 times larger than that of PFC(SC) film (29.8%). We speculate that the dense PFC(SC) film, which requires sufficient thickness to generate measurable fluorescence signal, could hinder the penetration and diffusion of DNT vapor, even cause the existence of unpenetrated and unquenched internal layer of the PFC(SC) film by DNT vapor, leading to lower responsiveness and sensitivity. On the other hand, since the spacing of cellobiose repeat unit was reported at approximately 1.04 nm, a large number of easily accessible cavities or pathways could be formed in the PFC@CNF film surface, which could benefit DNT vapor penetration into out layer of the film sensor. In addition, compared with the PFC@CNF film, the PFC@CELL paper showed moderate response sensitivity toward DNT vapor. Only about 54.5% quenching was observed after 600 s of exposure. It could be explained that for ordinary filter paper, there are more reactive sites (6 hydroxyl groups) on the cellobiose repeat unit than that for the CNF film (1 carboxyl group), which could build much denser grafting conjugated-polymer chains on the substrate, resulting in the partly-overlapping of PFC chain. As a result, the less accessible cavities or pathways would be formed in the PFC@CELL paper surface, which could prevent the diffusion of DNT molecules, leading to moderate response sensitivity.

The easily/less accessible cavities or pathways was further analyzed by introducing a parameter, the fraction of easily accessible

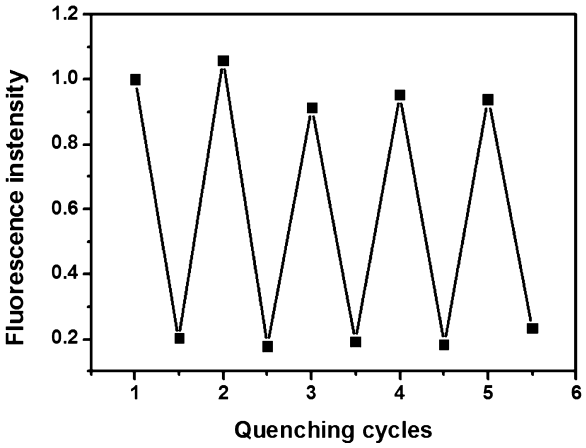

Fig. 6. The fluorescence quenching-recovery cycles test after the PFC@CNF film exposing to DNT for 60 s.

cavities on basis of the modified Stern–Volmer equation, which is approximately described by Eq (2) (Li, Kendig, & Nesterov, 2007):

$$\frac{I_0}{\Delta I} = \frac{1}{f_a} + \frac{1}{f_a K_{SV}^a t} \quad (2)$$

In Eq (2), I_0 is the fluorescence intensity in the absence of added quencher, $\Delta I = I_0 - I$ is the fluorescence intensity drop as a function of quencher, f_a is the fraction of easily accessible cavities, and K_{SV}^a is the Stern–Volmer constant for quenching inside these cavities. t is the exposure time.

The modified Stern–Volmer plots obtained for the PFC@CNF film, PFC@CELL paper and PFC(SC) film are shown in Fig. 5b. The fraction of easily accessible cavities f_a for the PFC@CELL paper and the PFC(SC) film were 0.57 and 0.30, respectively. However, for the PFC@CNF film, the f_a was up to be 0.97. Although the value of f_a is an approximate description of the PFC@CNF film surface topological structure, the much more numbers of easily accessible cavities or loose pathways indeed exist in the PFC@CNF film surface, which could benefit the penetration and diffusion of DNT molecules. In addition, the f_a of the PFC@CNF film is higher than that of molecularly imprinted CPs reported in literature which were prepared by sophisticated template-removal procedure producing material (Li et al., 2007). So, even without sophisticated polymer backbone/side-chain functionalization, the PFC@CNF film could display high responsiveness, which could be proposed to be an excellent candidate for detecting nitroaromatic vapor.

3.5. Reversibility of the quenching process

The reversibility of the sensing process was examined with DNT vapor as a representative nitroaromatic. After exposure to DNT vapor, the PFC@CNF film was washed with methanol several times and air-dried. The recovered film showed similar quenching efficiency when re-exposed to the DNT vapor (Fig. 6). Efficient quenching and recovery were obtained for practical utilities, and this implies that a good reversibility of the material and a highly fluorescence stability for the film against photobleaching could be achieved.

4. Conclusions

In conclusion, the functionalization of CNF film was carried out via specific grafting-to method of boronate-terminated CP chains at C-6 carboxyl groups on cellobiose repeat unit. The modified CNF film has been used as a fluorescent sensor for nitroaromatics detection. Based on the discussion of the estimated value of the fraction of easily accessible cavities (f_a of the PFC@CNF film is up to 0.97), the PFC@CNF film exhibits more rapid response toward DNT vapor than the SC(FC) film and FC@CELL paper. This demonstrated that the adopting of chemical assembly and specific reactive sites of the CNF film surfaces to build the loose cavities or pathways in the film sensor's out-layer could benefit the penetration and diffusion of DNT molecules.

References

Basabe-Desmonts, L., Reinhoudt, D. N., & Crego-Calama, M. (2007). Design of fluorescent materials for chemical sensing. *Chemical Society Reviews*, *36*(6), 993–1017.
Che, Y., Gross, D. E., Huang, H., Yang, D., Yang, X., Discekici, E., et al. (2012). Diffusion-controlled detection of trinitrotoluene: Interior nanoporous structure and low highest occupied molecular orbital level of building blocks enhance selectivity and sensitivity. *Journal of the American Chemical Society*, *134*(10), 4978–4982.
Feng, J., Li, Y., & Yang, M. (2010). Conjugated polymer-grafted silica nanoparticles for the sensitive detection of TNT. *Sensors and Actuators B: Chemical*, *145*(1), 438–443.
Follain, N., Marais, M.-F., Montanari, S., & Vignon, M. R. (2010). Coupling onto surface carboxylated cellulose nanocrystals. *Polymer*, *51*(23), 5332–5344.
Fukuzumi, H., Saito, T., Wata, T., Kumamoto, Y., & Isogai, A. (2009). Transparent and high gas barrier films of cellulose nanofibers prepared by TEMPO-mediated oxidation. *Biomacromolecules*, *10*(1), 162–165.
He, G., Zhang, G., Lue, F., & Fang, Y. (2009). Fluorescent film sensor for vapor-phase nitroaromatic explosives via monolayer assembly of oligo(diphenylsilane) on glass plate surfaces. *Chemistry of Materials*, *21*(8), 1494–1499.
Hirota, M., Furihata, K., Saito, T., Kawada, T., & Isogai, A. (2010). Glucose/glucuronic acid alternating co-polysaccharides prepared from TEMPO-oxidized native celluloses by surface peeling. *Angewandte Chemie-International Edition*, *49*(42), 7670–7672.
Holt, B. L., Stoyanov, S. D., Pelan, E., & Paunov, V. N. (2010). Novel anisotropic materials from functionalised colloidal cellulose and cellulose derivatives. *Journal of Materials Chemistry*, *20*(45), 10058–10070.
Isogai, A., Saito, T., & Fukuzumi, H. (2011). TEMPO-oxidized cellulose nanofibers. *Nanoscale*, *3*(1), 71–85.
Lan, A., Li, K., Wu, H., Olson, D. H., Emge, T. J., Ki, W., et al. (2009). A luminescent microporous metal-organic framework for the fast and reversible detection of high explosives. *Angewandte Chemie International Edition*, *48*(13), 2334–2338.
Li, J., Kendig, C. E., & Nesterov, E. E. (2007). Chemosensory performance of molecularly imprinted fluorescent conjugated polymer materials. *Journal of the American Chemical Society*, *129*(51), 15911–15918.
Long, Y., Chen, H., Yang, Y., Wang, H., Yang, Y., Li, N., et al. (2009). Electrospun nanofibrous film doped with a conjugated polymer for DNT fluorescence sensor. *Macromolecules*, *42*(17), 6501–6509.
Miao, J., Pangule, R. C., Paskaleva, E. E., Hwang, E. E., Kane, R. S., Linhardt, R. J., et al. (2011). Lysostaphin-functionalized cellulose fibers with antistaphylococcal activity for wound healing applications. *Biomaterials*, *32*(36), 9557–9567.
Narayanan, A., Varnavski, O. P., Swager, T. M., & Goodson, T., III. (2008). Multiphoton fluorescence quenching of conjugated polymers for TNT detection. *Journal of Physical Chemistry C*, *112*(4), 881–884.
Peterson, J. J., Willgert, M., Hansson, S., Malmstrom, E., & Carter, K. R. (2011). Surface-grafted conjugated polymers for hybrid cellulose materials. *Journal of Polymer Science Part A: Polymer Chemistry*, *49*(14), 3004–3013.
Saito, T., Kimura, S., Nishiyama, Y., & Isogai, A. (2007). Cellulose nanofibers prepared by TEMPO-mediated oxidation of native cellulose. *Biomacromolecules*, *8*(8), 2485–2491.
Tao, S., Li, G., & Zhu, H. (2006). Metalloporphyrins as sensing elements for the rapid detection of trace TNT vapor. *Journal of Materials Chemistry*, *16*(46), 4521–4528.
Thomas, S. W., III, Joly, G. D., & Swager, T. M. (2007). Chemical sensors based on amplifying fluorescent conjugated polymers. *Chemical Reviews*, *107*(4), 1339–1386.
Wang, Y., La, A., Ding, Y., Liu, Y., & Lei, Y. (2012). Novel signal-amplifying fluorescent nanofibers for naked-eye-based ultrasensitive detection of buried explosives and explosive vapors. *Advanced Functional Materials*, *22*(17), 3547–3555.
Wu, W., Ye, S., Huang, L., Xiao, L., Fu, Y., Huang, Q., et al. (2012). A conjugated hyperbranched polymer constructed from carbazole and tetraphenylethylene moieties: Convenient synthesis through one-pot "A_2+B_4" Suzuki polymerization, aggregation-induced enhanced emission, and application as explosive chemosensors and PLEDs. *Journal of Materials Chemistry*, *22*(13), 6374–6382.
Yang, J. S., & Swager, T. M. (1998). Fluorescent porous polymer films as TNT chemosensors: Electronic and structural effects. *Journal of the American Chemical Society*, *120*(46), 11864–11873.
Yang, Y., Turnbull, G. A., & Samuel, I. D. W. (2010). Sensitive explosive vapor detection with polyfluorene lasers. *Advanced Functional Materials*, *20*(13), 2093–2097.
Zhang, S., Lu, F., Gao, L., Ding, L., & Fang, Y. (2007). Fluorescent sensors for nitroaromatic compounds based on monolayer assembly of polycyclic aromatics. *Langmuir*, *23*(3), 1584–1590.
Zhu, W., Tao, S., Tao, C. A., Li, W., Lin, C., Li, M., et al. (2011). Hierarchically imprinted porous films for rapid and selective detection of explosives. *Langmuir*, *27*(13), 8451–8457.